

Langmuir–Blodgett film and second harmonic generation of a new type of amphiphilic non-linear optical bis-chromophore complex dye

Hui Li,^a Dejian Zhou,^a Chunhui Huang,^{a*} Jingmei Xu,^b Tiankai Li,^b Xinsheng Zhao^c and Xiaohua Xia^c

^aState Key Laboratory of Rare Earth Material Chemistry and Applications, Peking University, Beijing, 100871, China

^bInstitute of Photographic Chemistry, Academia Sinica, Beijing, 100082, China

^cDepartment of Chemistry, Peking University, Beijing, 100871, China

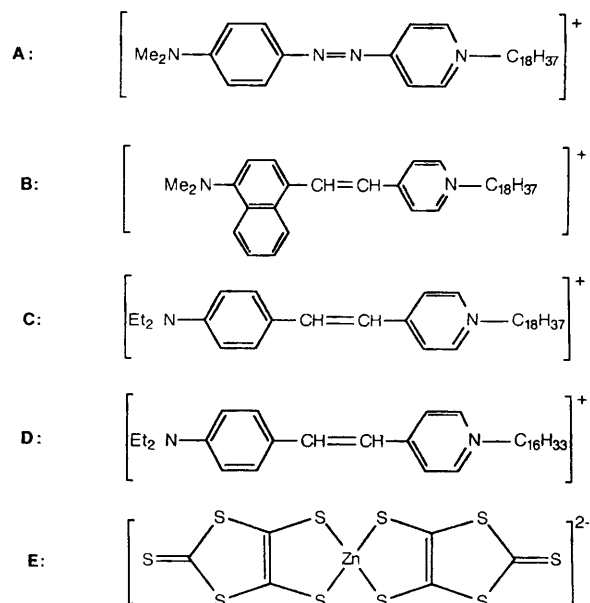
A bivalent zinc complex anion: bis(2-thione-1,3-dithiol-4,5-dimercapto)zinc, has been chosen to balance several non-linear optical (NLO) dye cations in the design and synthesis of a series of novel bis-chromophore complex dyes. The Langmuir film-forming properties of these new NLO complex dyes at the air/water interface, the stability and second-order non-linear optical properties of the monolayer and Langmuir–Blodgett multilayer films were investigated. Results show that both the film-forming properties and NLO coefficients were improved greatly when the zinc complex anion was incorporated into four types of NLO-active organic dyes.

Organic non-linear optical materials have received increasing attention owing to their wide transparent range, high non-linear optical (NLO) coefficient and extremely short response time and they may have various applications in the field of optical-signal processing, such as amplification, frequency conversion [*i.e.* second-harmonic generation (SHG)] and modulation.^{1–3} A non-centrosymmetric structure is a principal requirement for SHG. In organic materials this can be achieved *via* the Langmuir–Blodgett (LB) technique, which offers control of the structure at the molecular level. Among the reported non-linear materials, hemicyanines and azobenzenes have been extensively studied.^{4–8} The SHG of these films showed strong counter-anion dependence and is very sensitive to the extent of molecular aggregation. Mixed films, in which the dye molecules are interspersed with an inert phase, have been used to reduce aggregation and consequently enhance SHG, but in some cases, poor miscibility and phase separation of the inert molecules and NLO dyes was observed.⁵ Our previous papers have indicated that the introduction of a large lanthanide complex anion, which can be used as both spacer and counterion, into hemicyanine dyes can usually improve the film-forming performance and enhance SHG.^{9–11} To enhance the miscibility and thus further improve the second-order non-linearity, a different molecular architecture was designed for the dyes. In this paper, a bivalent zinc complex anion and several types of hemicyanine and azopyridinium NLO dyes were combined to form a new class of bis-chromophore NLO complex dyes. The bivalent zinc complex anion can be used as both counterion and spacer to give an ordered segregation of the chromophores. Furthermore, the combination of two chromophores into one molecule can increase the density of NLO-active moieties in a single layer. Therefore, this method can improve the film-forming properties of the NLO dyes and consequently enhance second susceptibility (χ^2) of the system while avoiding a red shift in UV–VIS absorption spectra. Scheme 1 shows the molecular structures of the eight different dyes studied in this paper.

Experimental

Materials

4-Dimethylaminonaphthaldehyde (>97%) was purchased from Aldrich. 4-Dimethylaminobenzaldehyde, 4-diethyl-



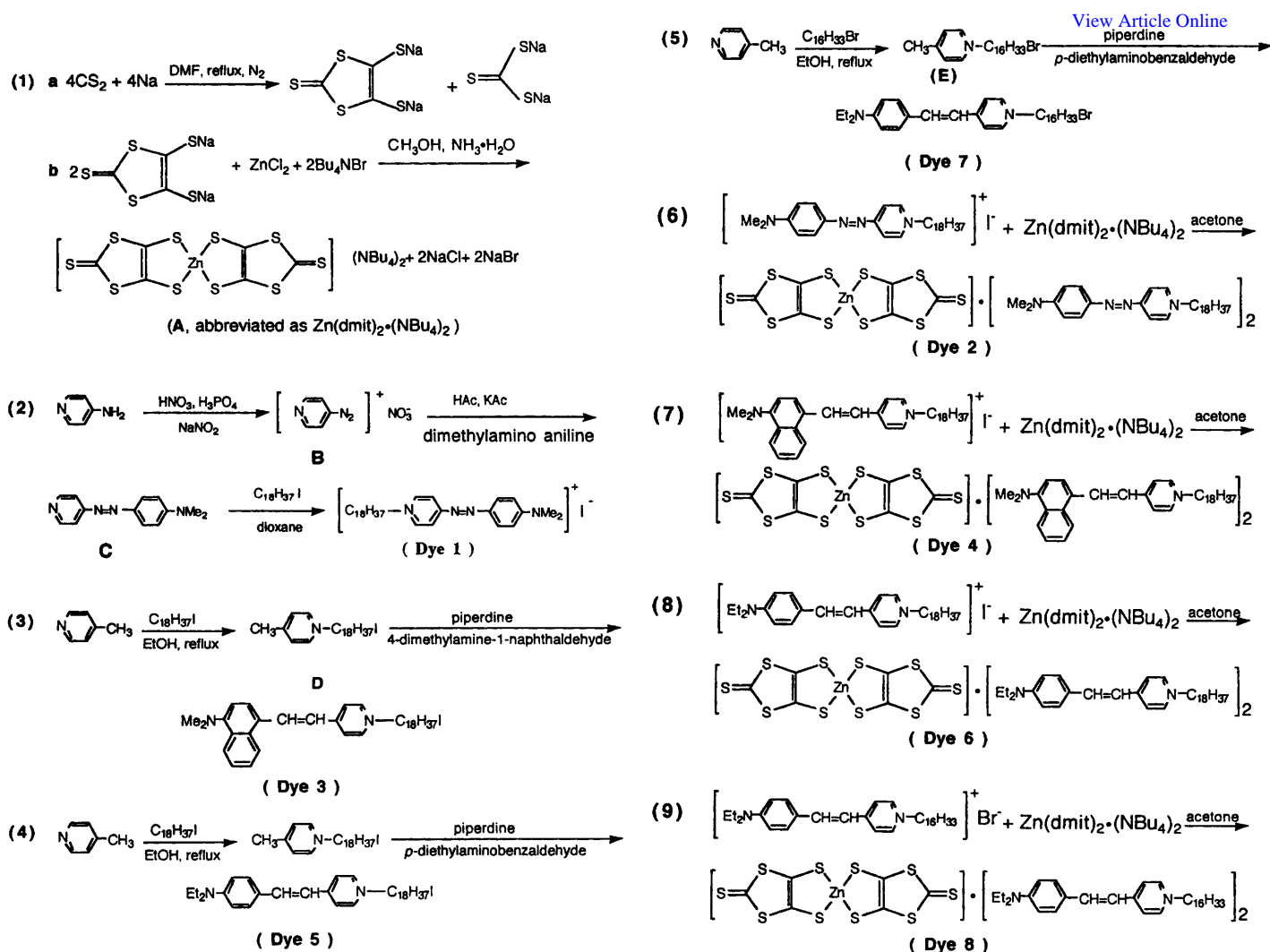
Dye 1: A1 Dye 2: A2E
Dye 3: B1 Dye 4: B2E
Dye 5: C1 Dye 6: C2E
Dye 7: D1 Dye 8: D2E

Scheme 1 Molecular structure of the complexes and their iodides and bromide

aminobenzaldehyde, 1-iodooctadecane, 1-bromohexadecane, 4-methylpyridine, 4-aminopyridine, tetrabutylammonium bromide, carbon disulfide and sodium metal were all AR grade products from Beijing Chemicals.

Synthesis

The synthetic procedures are shown in Scheme 2. The synthesis of bis(tetrabutylammonium) bis(2-thione-1,3-dithiol-4,5-dimercapto) zinc (compound A) was performed following the procedures of Steimecke¹² and Nakamura and co-



Scheme 2 Synthesis

workers.^{13,14} The other compounds were synthesized as follows.

4-(4-Dimethylaminophenylazo)pyridine (compound C). 4-Aminopyridine (3.6 g) was placed in a flask and resolved in a mixture of 20 ml 85% phosphoric acid and 10 ml 65–68% nitric acid, to which 2.8 g sodium nitrite was added slowly at a temperature below -5°C . Crushed ice (50 g) was then added and the resulting suspension was stirred for 1 h, a yellow solution (compound B) was obtained. To a solution of 40 g glacial acetic acid, 64 g potassium acetate and 56 g sodium carbonate, 8.4 ml 4-dimethylamino aniline was added, then compound B was added dropwise to the above solution at below 5°C . The resulting solution was stirred for 3 h and orange solids were collected by filtration and washed with water several times. The precipitates were recrystallized from acetone to obtain compound C as orange crystals (3.6 g, 50%).

***N*-Octadecyl-4-[(4-dimethylaminophenyl)azo]pyridinium iodide (dye 1).** 4-[(4-Dimethylaminophenyl)azo]pyridine (1.0 g) was placed in a flask and dissolved in 50 ml dioxane, to which 5.0 g 1-iodooctadecane was added. The mixture was refluxed for 4 h. When the solution was cooled, the precipitates were collected on a Buchner funnel then dissolved in benzene to reflux for 8 h. After evaporation of benzene, purple solid products were obtained. The crudes were washed with light petroleum ($30\text{--}60^\circ\text{C}$) then recrystallized four times from acetone–light petroleum. Dye 1 (80%) Found: C, 60.89; H, 8.43; N, 9.06. $\text{C}_{31}\text{H}_{51}\text{N}_4\text{I}$ requires C, 61.37; H, 8.47; N, 9.24.

***N*-Octadecyl-4-methylpyridinium iodide (compound D).** A mixture of 4-picoline (90 ml, 0.90 mol) and 1-iodooctadecane (190 g, 0.50 mol) in 150 ml ethanol was refluxed for 72 h. Most of the solvent was then driven off under reduced pressure in a water bath and the resulting solution was cooled in a refrigerator. When the temperature had reduced to 0°C , yellowish precipitates were filtered out and recrystallized three times from ethanol. Yield: 80%, mp $58\text{--}58.5^\circ\text{C}$.

(*E*)-*N*-Octadecyl-4-[2-(4-dimethylaminonaphthyl)ethenyl]pyridinium iodide (dye 3). To a mixture of 20 mmol compound D and 20 mmol 4-dimethylaminonaphthaldehyde in 30 ml absolute ethanol, 2 ml piperidine was added. The resulting solution was refluxed for 4 h with stirring. After cooling in a refrigerator, the precipitate was filtered out then recrystallized twice from ethanol. Yield: 60%. ^1H NMR δ_{H} [400 MHz, solvent CDCl_3 , tetramethylsilane (TMS) as standard; ppm], 0.84–0.88 (t, 3 H, CH_3), 1.20–1.28 [t, 30 H, $(\text{CH}_2)_{15}$], 1.93 (t, 2 H, + NCH_2CH_2), 2.95 (s, 6 H, NMe_2), 4.57–4.60 (t, 2 H, + NCH_2), 7.00 (d, 1 H, ethenyl), 7.20 (d, 1 H, ethenyl), 7.50 (m, 1 H, naphthyl ring), 7.60 (m, 1 H, naphthyl ring), 7.90 (d, 1 H, naphthyl ring), 8.10 (d, 2 H, pyridinium ring), 8.20 (d, H, naphthyl ring), 8.30 (d, 1 H, naphthyl ring), 8.40 (d, 1 H, naphthyl ring), 8.93 (d, 2 H, pyridinium ring). Found: C, 68.80; H, 8.80; N, 4.11. $\text{C}_{37}\text{H}_{55}\text{N}_2\text{I}$ requires C, 67.87; H, 8.31; N, 4.28.

(*E*)-*N*-Octadecyl-4-[2-(4-diethylaminophenyl)ethenyl]pyridinium iodide (dye 5). The synthesis was carried as for dye 3 from compound D and 4-diethylaminobenzaldehyde.

***N*-Hexadecyl-4-methylpyridinium bromide (compound E).** A mixture of 4-picoline (18.2 ml, 0.18 mol) and 1-bromohexadecane (65 ml, 0.21 mol) in 30 ml ethanol was refluxed for 24 h. After cooling in a refrigerator, the precipitate was filtered out and recrystallized twice from ethanol.

(E)-*N*-Hexadecyl-4-[2-(4-diethylaminophenyl)ethenyl]pyridinium iodide (dye 7). The synthesis was carried as for dye 5 from compound E and 4-diethylaminobenzaldehyde.

Bis[*N*-octadecyl-4-(4-dimethylaminophenylazo)pyridinium] bis(2-thione-1,3-dithiol-4,5-dimercapto) zinc (dye 2). Compound A (0.23 g, 0.24 mmol) and 0.30 g (0.48 mmol) dye 1 were dissolved in 20 ml acetone with heating. The resulting solution was refluxed for 10 min with stirring, then 40 ml water was added and the precipitate was filtered out and recrystallized twice from mixed solvents of acetone–water. Yield: 80%. $^1\text{H NMR } \delta_{\text{H}}$ (400 MHz, CDCl_3 , TMS as standard; ppm), 0.85–0.89 (t, 3 H, CH_3), 1.23–1.29 [d, 30 H, $(\text{CH}_2)_{15}$], 1.90 (d, 2 H, + NCH_2CH_2), 3.19 (s, 6 H, NMe_2), 4.42 (t, 2 H, + NCH_2), 6.73 (d, 2 H, phenyl ring), 7.90 (d, 2 H, phenyl ring), 7.97 (d, 2 H, pyridinium ring), 8.46 (d, 2 H, pyridinium ring). Found: C, 57.10; H, 7.35; N, 8.08; Zn, 4.94. $\text{C}_{68}\text{H}_{102}\text{N}_8\text{S}_{10}\text{Zn}$ requires C, 57.65; H, 7.21; N, 7.91; Zn, 4.62.

Bis(E)-*N*-octadecyl-4-[2-(4-dimethylaminophenyl)ethenyl]pyridinium bis(2-thione-1,3-dithiol-4,5-dimercapto) zinc (dye 4). Compound A (0.23 g, 0.24 mmol) and 0.33 g (0.50 mmol) dye 3 were dissolved in 20 ml acetone and 5 ml ethanol with heating. The resulting solution was stirred at 50 °C for 20 min, then 40 ml water was added and red solids were obtained. The crudes were recrystallized in acetone–water three times and red crystals were obtained. Yield: 70%. $^1\text{H NMR } \delta_{\text{H}}$ (400 MHz, solvent CDCl_3 , TMS as standard; ppm), 0.85–0.89 (t, 3 H, CH_3), 1.21–1.29 [t, 30 H, $(\text{CH}_2)_{15}$], 1.79–1.80 (d, 2 H, + NCH_2CH_2), 2.93 (s, 6 H, NMe_2), 4.14–4.18 (t, 2 H, + NCH_2), 7.00–7.04 (q, 2 H, ethenyl), 7.45–7.82 (m, 3 H, naphthyl ring), 7.84 (d, 2 H, pyridinium ring), 8.12–8.14 (d, 1 H, naphthyl ring), 8.18–8.19 (d, 2 H, pyridinium ring), 8.27–8.37 (m, 2 H, naphthyl ring). Found: C, 62.92; H, 6.70; N, 3.61; Zn, 4.29. $\text{C}_{80}\text{H}_{110}\text{N}_4\text{S}_{10}\text{Zn}$ requires C, 63.45; H, 7.27; N, 3.70; Zn, 4.32.

Bis(E)-*N*-octadecyl-4-[2-(4-diethylaminophenyl)ethenyl]pyridinium bis(2-thione-1,3-dithiol-4,5-dimercapto) zinc (dye 6). The synthesis was carried out as for dye 4 from compound A and dye 5. Found: C, 62.38; H, 8.00; N, 3.74; Zn, 4.70. $\text{C}_{76}\text{H}_{114}\text{N}_4\text{S}_{10}\text{Zn}$ requires C, 62.15; H, 7.77; N, 3.82; Zn, 4.46.

Bis(E)-*N*-hexadecyl-4-[2-(4-diethylaminophenyl)ethenyl]pyridinium bis(2-thione-1,3-dithiol-4,5-dimercapto) zinc (dye 8). The synthesis was carried out as for dye 4 from compound A and dye 7. Found: C, 60.94; H, 7.56; N, 3.69. $\text{C}_{74}\text{H}_{110}\text{N}_4\text{S}_{10}\text{Zn}$ requires C, 61.23; H, 7.55; N, 3.96.

Langmuir film formation and deposition

Monolayer experiments were performed on a British NIMA technology Langmuir–Blodgett trough. For the control and evaluation of the experiment, a Commodore computer was used. The Langmuir films were spread from their CHCl_3 solutions at a concentration of about $5 \times 10^{-4} \text{ mol l}^{-1}$ onto a pure water subphase ($20.0 \pm 0.1^\circ\text{C}$, pH 5.60). After vaporization of CHCl_3 , the surface pressure–area (π – A) isotherms were recorded at a compression rate of 15 mm min^{-1} . The Langmuir films were deposited as Z-type (up stroke only) or Y-type (both up and down stroke) onto hydrophilically pretreated substrates^{15,16} at a deposition rate of 5 mm min^{-1} at constant surface pressure, as listed in Table 1.

Optical characterization

The UV–VIS spectra of monolayers and LB multilayers on quartz plates were recorded on a Shimadzu UV-3100 spectrophotometer, using black quartz as a reference. IR spectra were measured on a Nicolet 7199B FT-IR spectrometer. X-Ray photoelectron spectra were taken on ESCA LAB-5 system at a constant pass energy of 20 eV. The excitation source was Al-K α radiation (1486 eV) and the chamber pressure was $8 \times 10^{-4} \text{ Pa}$. For calibration purposes, a C 1s line was set at 286.4 eV as the standard. Low-angle X-ray diffractograms of a 29-layer LB film of dye 2 on a quartz plate were obtained on a Rigaku D/Max-3B diffractometer, using Cu-K α radiation ($\lambda = 0.154 \text{ nm}$).

SHG measurement

The SHG was measured in transmission with a Y-cut quartz plate as a reference ($d_{11} = 1.2 \times 10^{-9} \text{ esu}$).^{9–11} The peak power of the Nd:YAG laser beam ($\lambda = 1064 \text{ nm}$) was 5.1 MW cm^{-2} with a pulse duration of 10 ns and a repetition rate of 10 Hz. A $1/4 \lambda$ plate and a Glan-Taylor polarizer were used to vary the polarization direction of the laser beam. The laser light, linearly polarized either parallel (p) or perpendicular (s) to the plane of incidence, was directed at an incidence angle of 45° onto the vertically mounted sample. A set of 1064 nm filters and a monochromator were used to ensure that only second-harmonic light was detected. The second-harmonic signals were detected by a photomultiplier. The average-output signals were recorded on a figurized storage recorder (HP 54510A). To compare the SHG signals of the dyes, we measured the SHG of the samples in the same experiment and all the results were repeated at least twice.

Results and Discussion

Spreading behaviour

The surface pressure–area isotherms of the eight dyes are shown in Fig. 1. The parameters of the monolayers are listed in Table 1. As can be seen from Fig. 1, dye 1 shows good

Table 1 Parameters of the monolayer films

molecule	l /Å ^a	collapse pressure /mN m ⁻¹	limiting area /Å ²	solid-phase slope /mN mÅ ⁻²	deposition pressure /mN m ⁻¹
1	29.1	44.3	57.4	1.76	35
2	31.0	50.0	81.2	4.03	35
3	26.2	36.5	162.0	0.44	25
4	30.5	49.8	93.8	1.50	35
5	26.5	30.0	161.4	0.36	25
6	32.2	49.8	78.7	1.92	35
7	28.7	33.4	142.0	0.56	25
8	31.5	47.3	83.4	1.48	35

^a Single thickness obtained by molecular modelling.⁷

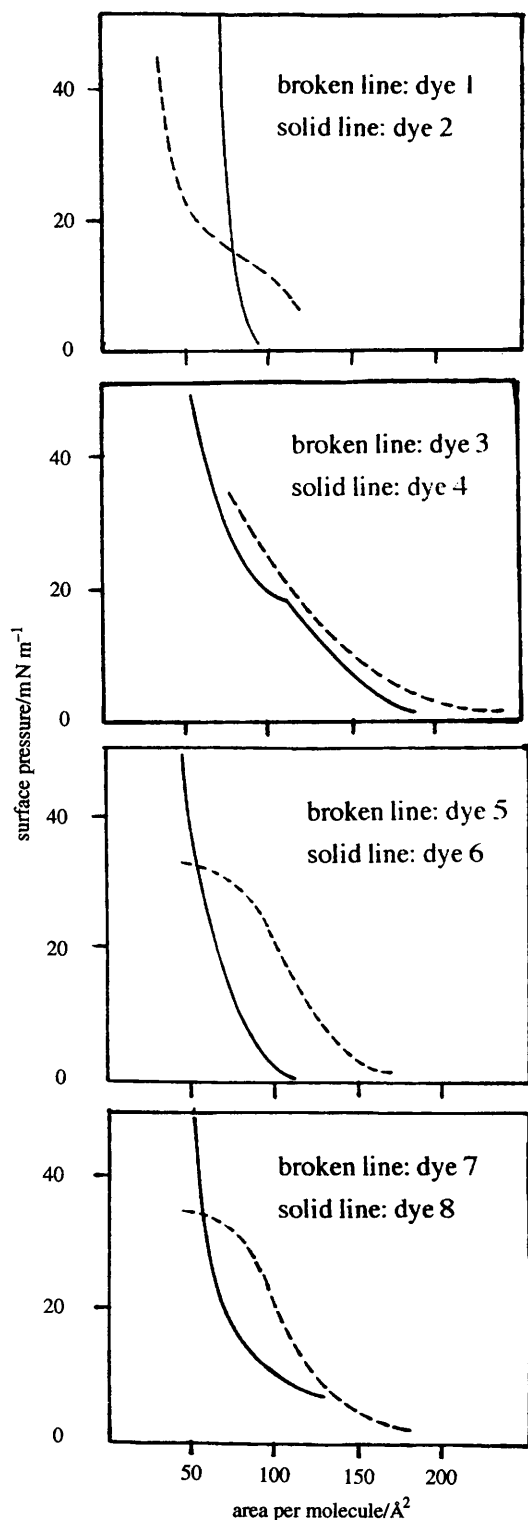
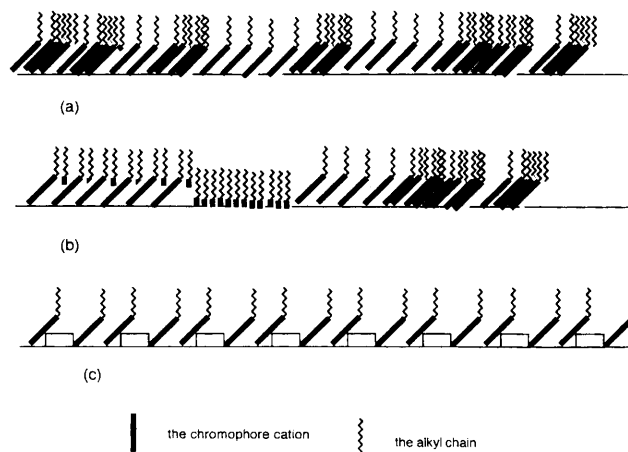


Fig. 1 Surface pressure–area isotherms of the eight dye monolayers at the air/water interface

film-forming properties with relatively high collapse surface pressure (44 mN m^{-1}) and a large condensed region slope (1.76 mN mÅ^{-2}). However, the film-formation properties of its assembled zinc complex dye [dye 2, Fig. 1(a) solid line] are even better with a larger condensed region slope (4.03 mN mÅ^{-2}) and a higher collapse surface pressure (50 mN m^{-1}). Observation shows that the combination of two univalent azo dyes (dye 1) using a bivalent zinc complex anion can further improve the film-forming properties although the dye itself has good film-formation properties. Dyes 3, 5 and 7 show poor film-formation properties which can also be improved by

this kind of combination method. For example, the condensed region slope and collapse pressure of the zinc complex dye (6) are 1.92 mN mÅ^{-2} and 50 mN m^{-1} , while those for the dye iodide (5) are only 0.36 mN mÅ^{-2} and 30 mN m^{-1} .

Mixed films, in which the dye molecules could be interspersed with an inert phase have been used to improve film-forming properties and reduce aggregation,⁷ but these films have the potential disadvantage of phase separation [Scheme 3(b)]. An alternative method of chromophore segregation was explored using a spacer (zinc complex anion) as part of the molecule. This method can greatly improve the film forming properties without the danger of phase separation.



Scheme 3 Possible molecular arrangement of the dyes on substrates: (a) in monolayers of pure organic dyes there is molecular aggregation which may affect the NLO properties of the film considerably; (b) mixed films in which the dye molecules are interspersed with an inert phase have been used to reduce the aggregation and hence enhance the SHG, but they suffer from phase separation; (c) in zinc complex dyes the large bivalent zinc complex anion can be used as both counterion and spacer to give an ordered segregation of the chromophore and greatly enhance SHG.

The limiting area per molecule of dye 2 (81.2 Å^2), obtained by extrapolation of the condensed region in the isotherm to $\pi = 0$, is larger than that of dye 1 (57.4 Å^2). However, it is not a rule for other complex dyes (4, 6 and 8). For example, the limiting area per molecule of the hemicyanine iodide (3) is 1.62 nm^2 , while that for its combined zinc complex dye (4) is only 0.94 nm^2 . A possible explanation is that the chromophore cations in dye 4 can arrange in a more orderly manner and closer together than those in dye 3. This is verified by SHG measurement which indicates that the tilt angle of the chromophore is less than that of the corresponding dye halides (except for dye 2). All these facts indicate that the incorporation of the zinc complex anion can improve the film-forming properties.

Stability of the Langmuir films

The stabilities of the Langmuir films of the eight dyes were studied by compressing and maintaining the Langmuir films at constant surface pressure, and the film area in the LB trough was plotted as a function of time. Typical examples of dye 1 and its combined zinc complex dye (2) are shown in Fig. 2. The data for other dyes are listed in Table 2. A parallel line was obtained for dye 2 [Fig. 2(a)], indicating that its film area can be kept at a constant value. However, the film area of dye 1 vibrates by a few percent at 35 mN m^{-1} . This indicates the Langmuir film of dye 2 is more stable than that of dye 1, although they both have good film-forming properties. The behaviour of other dyes is different from dyes 1 and 2. As given in Table 2, the film area of other dyes gradually decreases as a function of time at 25 mN m^{-1} . This may be

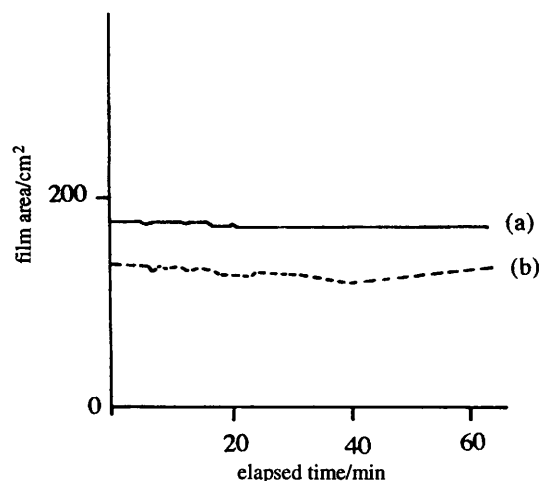


Fig. 2 Film area in the LB trough at a constant surface pressure of 35 mN m^{-1} as a function of time: (a) dye 1; (b) dye 2

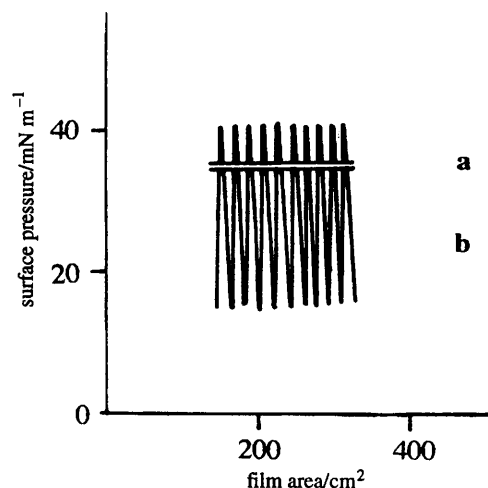


Fig. 3 The transfer of Y-type LB multilayer of dye 2

due to both of the two terminals in these molecules having some degree of hydrophobicity, so that molecules cannot pack together as closely as those in dye 1 or 2. However, the area decrease in the dye halides is much greater than that of its corresponding zinc complex dyes. A possible explanation is that the complex dyes have a much greater molecular mass than their dye halides.

We consider this to be a very significant performance for materials used in the LB technique, particularly that of making LB multilayers.

The π - A isotherms of dye 2 at different temperatures (12.5, 16.5, 26.5 and 30°C) were also studied. The isotherms are almost the same, indicating the stability of the Langmuir films. We can therefore conclude that the combination of the azo dye (1) with the zinc complex anion can improve the stability of the Langmuir films at the air/water interface.

Formation of LB films

The transfer of the Langmuir film to form LB multilayers (Y-type) was investigated for dye 2. The surface pressure (curve a) and the area change of the film during deposition (curve b) are shown in Fig. 3. It shows an excellent Langmuir-film transfer with the same transfer ratio of 1.09 at a constant surface pressure of 35 mN m^{-1} . In addition, the transfer ratio was maintained at approximately unity as the layer number increased up to at least 20 layers. In contrast, the transfer of the Langmuir film of dye 1 became difficult as the layer number increased.

UV-VIS spectra

UV-VIS spectra of the monolayers are shown in Fig. 4. It can be seen that they all exhibit the characteristic absorption bands of the chromophore cations in the visible region (550 nm for dye 1, 570 nm for 2, 440 nm for dyes 3 and 4 and 470 nm for dyes 5, 6, 7 and 8). These bands were usually assigned to the $\pi \rightarrow \pi^*$ electron transfer of the chromophores. The characteristic $\pi \rightarrow \pi^*$ electron-transfer absorption band of the zinc complex anion is *ca.* 400 nm and very weak, so it gives little effect on the characteristic absorption bands of the dye cations in the visible region when they are combined together to form one compound. The absorption band at *ca.* 280 nm of the zinc complex monolayer is stronger than that of its corresponding dye halides. The absorbance of dye 2 at 280 nm and 570 nm was plotted as a function of the layer number giving straight lines (Fig. 5). This indicates that the Langmuir film was effectively transferred, in good agreement with its transfer ratio which was always maintained around unity. In addition, the LB multilayers of dye 2 are long-term stable, no changes could be observed in the UV-VIS spectra.

IR spectra

The IR spectrum of a 14-layer LB film of dye 2 on a CaF_2 substrate is similar to its powder complex (Fig. 6), but differences can also be observed. For example, in the 14-layer LB film, the peak intensity at *ca.* 1600 cm^{-1} is weaker than that of *ca.* 2900 cm^{-1} , contrary to that in the powder complex

Table 2 Area changes of dye Langmuir films with time at 25 mN m^{-1}

time /min	film area/cm ²					
	dye 3	dye 4	dye 5	dye 6	dye 7	dye 8
0	448.2	357.0	536.0	345.4	478.0	382.5
2	442.8	352.0	524.8	339.0	466.6	376.5
5	438.4	346.0	515.3	332.8	455.7	372.0
10	431.6	339.1	503.5	326.3	443.5	368.0
15	424.8	334.5	494.8	321.7	434.5	365.9
20	419.1	331.0	487.3	318.2	427.8	364.3
25	413.5	328.2	480.8	315.3	422.0	363.5
30	408.8	326.0	474.8	313.0	415.3	362.8
35	404.2	324.4	469.4	310.6	409.0	362.6
40	399.8	322.8	464.2	308.7	403.6	362.4
45	395.6	321.7	459.6	307.2	398.6	362.2
50	391.6	320.0	455.0	305.2	394.8	362.1
55	387.8	319.0	450.8	303.5	390.8	362.0
60	383.9	318.0	446.7	302.5	387.2	362.0

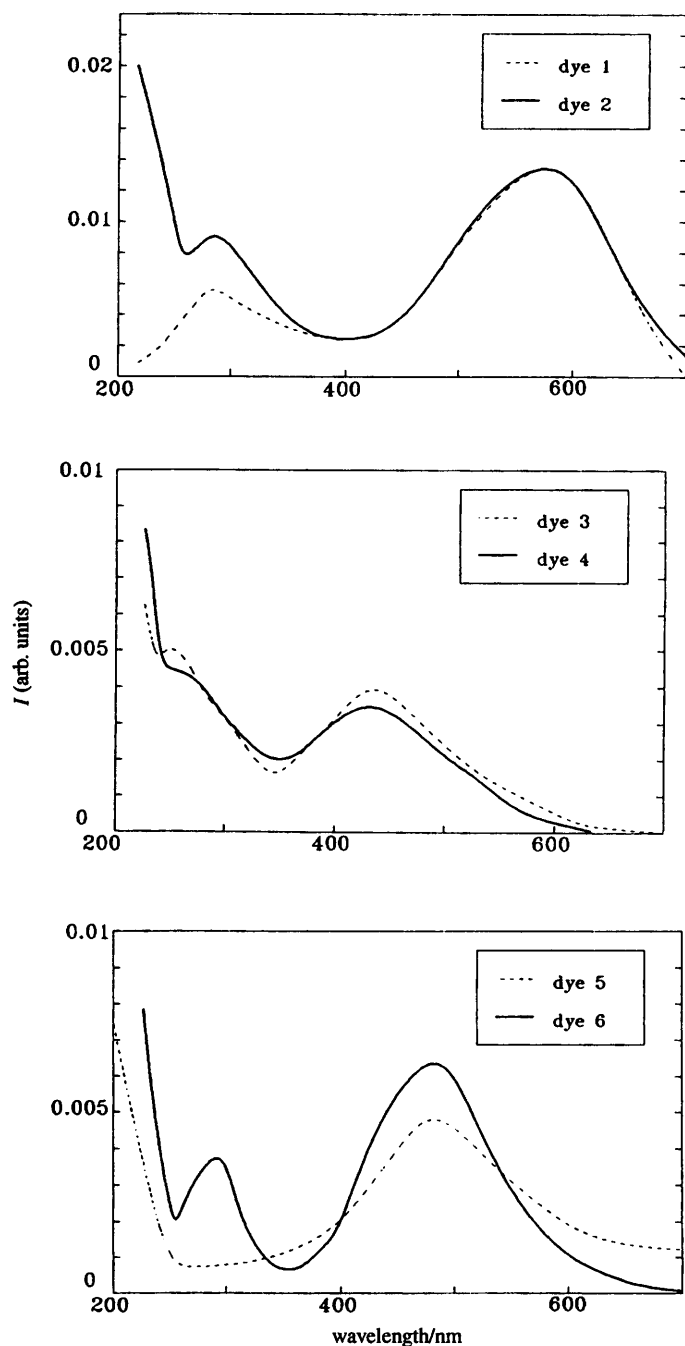


Fig. 4 UV-VIS spectra of dye monolayers on fused quartz substrates

(Fig. 6). We believe that this is due to the different molecular arrangement in the LB film and the powder complex. Some IR peaks are assigned as follows. The peaks at 2925 and 2860 cm^{-1} are the asymmetric and symmetric stretching of the CH_2 group in the alkyl long chains. The peak at 1600 cm^{-1} may be assigned to C-H bending. The peak at 1430 cm^{-1} (shoulder) may be assigned to N=N bond stretching and that at 1330 cm^{-1} (shoulder) may be assigned to Ar-N stretching.

Low-angle X-ray diffraction

The low-angle X-ray diffractogram of a 29-layer Y-type LB film of dye 2 on a glass plate is shown in Fig. 7. A well defined film structure is revealed by contrasting the regular diffraction peaks from the LB film with that from its polycrystalline powder complex. The diffraction peaks at 2θ of 3.0, 4.5 and 6.0° are assigned to (002), (003) and (004) Bragg diffraction,

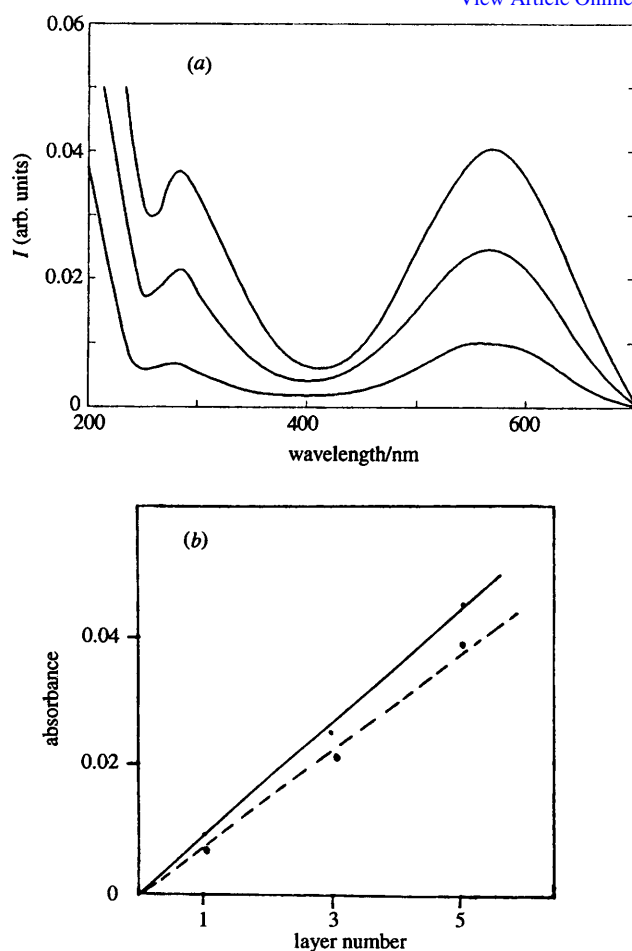


Fig. 5 (a) UV-VIS spectra of the LB films of dye 2 at (top to bottom) 5, 3 and 1 layers. (b) Absorbance of dye 2 at 570 nm (solid line) and 280 nm (broken line) vs. layer number.

respectively. This yields an average layer spacing of 59 Å according to the Bragg equation. Thus a single-layer film thickness of 29.5 Å is obtained based on the Y-type structure of the film (one layer spacing contains two single layers). The single-layer film thickness is less than the value calculated from molecular modelling (31 Å), suggesting that the fatty long chains may insert into each other within the double layers. A 29-layer LB film on a CaF_2 plate stored for 60 days at room temperature also exhibits similar diffraction peaks at 2θ of 3.0, 4.5 and 6.0°, which may be assigned to (002), (003) and (004) diffraction. A single-layer film thickness of 29.5 Å was again obtained, showing that the LB films have good stability with time.

X-Ray photoelectron spectra

The X-ray photoelectron spectra for both the powder complex of dye 2 and a three-layer LB film (Y-type) on a glass substrate at different taken-off depths exhibit characteristic peaks with a binding energy of Zn, N, S and C elements (Table 3). The electron inelastic free path was estimated according to ref. 13. From Table 3, we can see that the atomic ratios change greatly with the taken-off depth. For a taken-off depth of 10 Å, no zinc atoms can be detected. Most of the detected atoms are carbon, other atoms such as sulfur or nitrogen are very few. However, when the taken-off depth increases to 20 Å, zinc atoms still cannot be detected, but the atom ratios of sulfur and nitrogen increase considerably. When the taken-off depth changes to 40 Å, all of the atoms can be detected and the atom ratios for all of the elements are very close to those in the powder samples. This verifies that the LB film has an

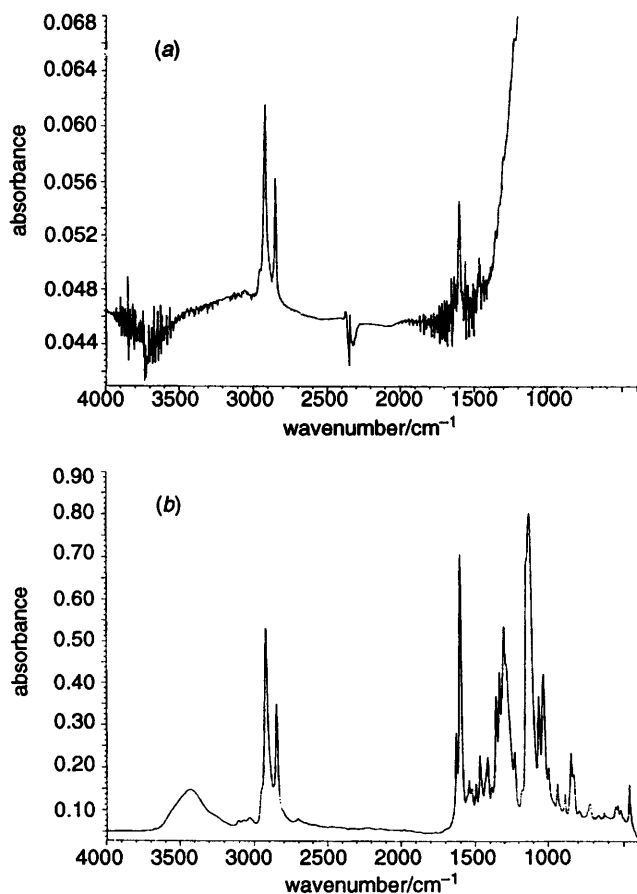


Fig. 6 FTIR spectra of a 14-layer LB film of dye 2 on a CaF_2 plate (a) and its powder complex (b)

ordered layer structure, reflecting the good quality of the films.¹⁷

SHG study

On the assumption that the chromophores have a common tilt angle ϕ with a random azimuthal distribution, and that the second-order molecular hyperpolarizability (β) is dominated by the component along the intramolecular donor- π -acceptor axis, according to ref. 4 and 7, the following equations can be obtained:

$$\frac{I_{2\omega}^{p \rightarrow p}}{I_{2\omega}^{s \rightarrow p}} = \frac{(\chi_{zzz}^2 \sin^3 \theta + 3\chi_{zxx}^2 \sin \theta \cos^2 \theta)^2}{(\chi_{zxx}^2 \sin \theta)^2} \quad (1)$$

$$\chi_{zzz}^2 = Nf_{2\omega}(f_{\omega})^2\beta \cos^3 \phi \quad (2)$$

$$\chi_{zxx}^2 = 0.5Nf_{2\omega}(f_{\omega})^2\beta \cos \phi \sin^2 \phi \quad (3)$$

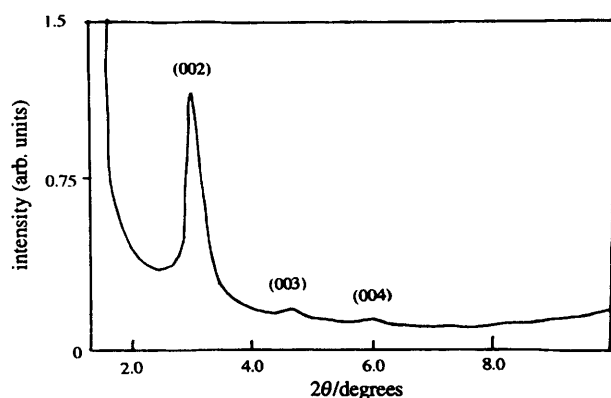


Fig. 7 Low-angle X-ray diffractogram of a 29-layer LB film of dye 2 on a glass substrate

Table 3 Atom ratios of Zn, N and S : C element at different taken-off depths

taken-off depth /nm	Zn : C (%)	N : C (%)	S : C (%)
1.0	0	0.22	0.26
2.0	0	4.0	2.8
4.0	0.95	4.8	9.7
powder	0.85	5.3	11.2

where N is the number of the molecules per unit volume, θ is the angle of the laser beam towards the surface normal of the films (45° in this study), $f_{\omega, 2\omega} = [(n_{\omega, 2\omega})^2 + 2]/3$, is a local-field-correction factor, $n_{2\omega}$ and n_{ω} are the refractive indices at second-harmonic frequencies (532 nm) and fundamental frequencies (1064 nm), respectively, ϕ is the tilt angle of the chromophore relative to the normal of the film surface and $I_{2\omega}^{p \rightarrow p}$ is the p-polarized double frequency signal intensity with p-polarized incidental fundamental light, $I_{2\omega}^{s \rightarrow p}$ is p-polarized double frequency signal intensity with s-polarized incidental fundamental light. The tilt angle ϕ can be calculated by eqn. (4) which is obtained by a combination of eqn. (1)–(3).

$$\tan \phi = \frac{\sin \phi}{\cos \phi} = \left[\left(\frac{I_{2\omega}^{p \rightarrow p}}{I_{2\omega}^{s \rightarrow p}} \right)^{1/2} - \frac{3}{2} \right]^{-1/2} \quad (4)$$

In calculation, we assume that $n_{2\omega} = 1.8$ for dyes 1 and 2, $n_{2\omega} = 1.5$ for the other dyes and $n_{\omega} = 1.5$.¹⁸ By comparing the SH signals ($I_{2\omega}^{p \rightarrow p}$) with that from the quartz reference ($d_{11} = 1.2 \times 10^{-9}$ esu),⁷ the second-order susceptibility (χ^2) and the tilt angle ϕ can be evaluated and they are given in Table 4.

It is apparent that the second-order non-linearity of the monolayers is counter-anion dependent, and that the susceptibility (χ^2) of the complex dyes is enhanced two to three times compared with their corresponding azopyridinium and hemicyanine halides. The stronger signals are not attributed to resonant enhancement, since the introduction of the metal complex anion to the chromophores gives little change to the absorption spectra in visible light (the characteristic absorption peak of the zinc complex is near 400 nm and weak). All the monolayers of the zinc complex dyes show almost the same λ_{max} and the same overlap at the harmonic wavelength (532 nm) as their corresponding dye halides in UV-VIS spectra. The zinc complex anion shows no SH signal due to its centrosymmetric structure,^{12–14} so the improvement in SHG is not due to the non-linearity of the complex anion. It has been reported that the SHG of the dye films is sensitive to the extent of molecular aggregation (Scheme 3). In this work, an alternative method of chromophore segregation was explored using a spacer (zinc complex anion) that constitutes part of the molecule. In the zinc complex dyes (2, 4, 6 and 8), the two fatty alkyl chains of the two chromophores should pack side-by-side to the zinc complex anion because of the static electronic force. This may arrange the dye molecules in a more orderly manner on the substrates. On the other hand, the dipolar-dipolar interaction of the chromophore ions may be

Table 4 Comparison of the susceptibility (χ^2), tilt angle (ϕ) and λ_{max}

dye	$\chi^2 / 10^{-6}$ esu	ϕ /degrees	λ_{max} /nm
1	1.3	41	550
2	2.3	44	570
3	0.21	52	445
4	0.64	35	440
5	0.22	51	470
6	0.55	26	460
7	0.17	43	470
8	0.52	30	475

effectively restrained by the large complex anion so that the SHG is enhanced. Furthermore, the combination of two chromophores into one molecule may increase the density of NLO-active moieties in a single layer.

Comparing the SHG from the monolayers of the extensively studied hemicyanine halides (dyes 5 and 7), the monolayer of the zinc-complex-assembled dyes (4) shows much stronger SH intensities (about 10 times). There is very little resonance enhancement, since the absorption of dye 4 is much weaker than that of dye 5 or 7 at the harmonic frequency (532 nm), thus the resonant enhancement is not the main factor. The improved SH signal is probably due to the orderly arrangements of the chromophores using the bulk bivalent zinc complex anion. Another possible cause is that dye 4 shows much better film-forming properties than dye 5 or 7.

It is also noteworthy that the SH intensity of dye 2 is much stronger (about 100 times) than that of hemicyanine iodide (dye 5) or bromide (dye 7). This may be partly due to the overlap of the second-harmonic ($\lambda_{2\omega}$, 532 nm) and absorption bands (λ_{\max} , 570 nm, with a half width at half maximum of 85 nm) and partly due to the introduction of the zinc complex anion.

Conclusion

Two mono-charged NLO chromophore cations have been combined with a bivalent zinc complex anion to give a series of novel amphiphilic bis-chromophore dyes. Based on this ideal, a series of more homogeneous and stable LB films with high optical quality have been obtained. A non-resonant-enhanced second-harmonic generation from the monolayers of hemicyanines and azopyridinium dyes has been observed by the replacement of the halide anion with the zinc complex anion, which can be used as both counterion and spacer. More recently, we found that SHG quadratic enhancement with film thickness (layer number) could be obtained from a similar structure of the zinc complex dyes. The complex dyes may therefore qualify for possible non-linear optical applications. Previously, there have been few successful examples of materials with both high non-linearity and good additivity.¹⁸ This work is in progress.

The authors thank the Climbing Program (A National Fundamental Research Key Project of China) and the National Natural Science Foundation of China for the financial support of this project.

References

- 1 P. N. Prasad and D. J. Williams, *Introduction to Nonlinear Optical Effects in Molecules and Polymers*, Wiley, New York, 1991.
- 2 R. A. Hann and D. Bloor, *Organic Materials for Non-linear Optics*, Royal Society of Chemistry, London, 1989.
- 3 D. S. Chemla and J. Zyss, *Nonlinear Optical Properties of Organic Molecules and Crystals*, Academic Press, Orlando, FL, 1987, vol. 1 and 2.
- 4 D. Lupo, W. Prass, U. Scheunemann, A. Laschewsky, H. Ringsdorf and I. Ledoux, *J. Opt. Soc. Am. B: Opt. Phys.* 1988, **5**, 300.
- 5 G. J. Ashwell, E. J. C. Dawnay, A. P. Kuczynski and P. J. Martin, *SPIE Int. Soc. Opt. Eng.*, 1991, **1361**, 589.
- 6 G. J. Ashwell, *Mater. Res. Soc. Symp. Proc.*, 1992, **247**, 787.
- 7 G. J. Ashwell, R. C. Hargreaves, C. E. Baldwin, G. S. Bahra and C. R. Brown, *Nature (London)*, 1992, **357**, 393.
- 8 I. R. Marosky, L. F. Chi, D. Mobius, R. Steinhoff, Y. R. Shen, D. Dorsch and B. Rieger, *Chem. Phys. Lett.*, 1988, **147**, 420.
- 9 D. J. Zhou, C. H. Huang, K. Z. Wang, G. X. Xu, L. G. Xu, T. K. Li, X. S. Zhao and X. M. Xie, *Langmuir*, 1994, **10**, 1910.
- 10 K. Z. Wang, C. H. Huang, G. X. Xu, Y. Xu, Y. Q. Liu, D. B. Zhu, X. S. Zhao, X. M. Xie and N. Z. Wu, *Chem. Mater.*, 1994, **6**, 1986.
- 11 C. H. Huang, K. Z. Wang, G. X. Xu, X. S. Zhao, X. M. Xie, Y. Xu, Y. Q. Liu, L. G. Xu and T. K. Li, *J. Phys. Chem.*, 1995, **99**, 14397.
- 12 G. Steimecke, *Phosphorus Sulfur Silicon Relat. Elem.*, 1979, **17**, 49.
- 13 T. Nakamura, H. Tanaka and N. Watsnsbe, *Chem. Lett.*, 1989, 1667.
- 14 T. Nakamura, H. Tanaka and M. Yoneichiro, *Synth. Met.*, 1988, **27**, 13601.
- 15 L. B. Gan, D. J. Zhou, C. P. Luo, C. H. Huang, T. K. Li, J. Bai, X. S. Zhao and X. H. Xia, *J. Phys. Chem.*, 1994, **98**, 12459.
- 16 D. J. Zhou, L. B. Gan, C. P. Luo, H. S. Tan, C. H. Huang, Z. F. Liu, Z. Y. Wu, X. S. Zhao, X. H. Xia, F. Q. Sun, S. B. Zhang, Z. J. Xia and Y. H. Zou, *Chem. Phys. Lett.*, 1995, **235**, 548.
- 17 H. J. Chen, X. D. Chai, K. Tian, Q. Wei and T. J. Li, *Chem. J. Chin. Univ.*, 1991, **12**, 524.
- 18 G. J. Ashwell, P. D. Jackson and W. A. Crossland, *Nature (London)*, 1994, **368**, 438.

Paper 5/08039H; Received 11th December, 1995